Interactions of the A1 Heterogeneous Nuclear Ribonucleoprotein and Its Proteolytic Derivative, UP1, with RNA and DNA: Evidence for Multiple RNA Binding Domains and Salt-Dependent Binding Mode Transitions†

Steven G. Nadler,*,‡,⊥ Barbara M. Merrill,‡ William J. Roberts,‡ Kathleen M. Keating,‡ Michael J. Lisbin,‡ Stanley F. Barnett,‡ Samuel H. Wilson,§ and Kenneth R. Williams∥

Department of Molecular Biophysics and Biochemistry, Yale University, and Howard Hughes Medical Institute, New Haven, Connecticut 06510, and Laboratory of Biochemistry, National Cancer Institute, National Institutes of Health, Bethesda, Maryland 20892

Received October 3, 1990; Revised Manuscript Received December 24, 1990

ABSTRACT: The 319-residue A1 heterogeneous nuclear ribonucleoprotein is the best studied of the group of major or core mammalian hnRNP proteins that bind pre-mRNA immediately following transcription. Circular dichroism studies suggest that binding of A1 and its proteolytic fragment, UP1 (residues 1–195), to nucleic acids results in an unstacking of the bases of poly(A). On the basis of poly[d(A-T)] and poly[r(A-U)] melting studies, both A1 and UP1 are helix-destabilizing proteins. Titrations of A1 and UP1 with poly(A), poly(U), and poly[d(T)] suggest that these two proteins do not bind with significant base specificity. A previous study indicated that A1, which contains a glycine-rich COOH terminus (residues 196–319) not present in UP1, binds cooperatively to polynucleotides while UP1 does not [Cobianchi et al. (1988) *J. Biol. Chem. 263*, 1063–1071]. Here we confirm this latter finding and demonstrate that the cooperativity parameter for A1 binding, which has a value of about 35 for binding to both single-stranded RNA and DNA, is insensitive to the NaCl concentration at least up to 0.4 M. In contrast to the cooperativity parameter, the occluded site size for A1 binding to RNA is salt dependent and increases from about 14 to 28 upon increasing the NaCl concentration from 25 to 250 mM. This variation in site size is best explained by assuming that A1 can interact with nucleic acids via at least two different binding modes. Both A1 and UP1 have higher affinity for single-stranded as opposed to double-stranded nucleic acids and bind preferentially to single-stranded RNA as compared to DNA. Comparative studies on the binding of A1 versus UP1 to poly[r(ϵA)] demonstrate that in addition to cooperative protein/protein interactions, the glycine-rich COOH-terminal domain of A1 is also directly involved in protein/nucleic acid interactions. These conclusions are directly confirmed by studies on a 48-residue synthetic peptide corresponding to residues 260–307 in A1. In 10 mM NaCl, this peptide has an intrinsic affinity of 1.5×10^6 M^{-1} for poly[r(ϵA)] and a cooperativity parameter of about 30. The similar cooperativity parameters for A1 and this synthetic peptide analogue suggests that most of the structural determinants necessary for A1/A1 cooperative protein interactions are within residues 260–307 in A1. Together these studies demonstrate that the UP1 and glycine-rich COOH-terminal domains of A1 make an approximately equal and independent contribution to the overall free energy of A1 binding to single-stranded RNA.

Immediately following transcription, nascent heterogeneous RNA (hnRNA) is complexed in the nucleus with six major proteins (Beyer et al., 1977) that together form a ribonucleoprotein particle (hnRNP)[1] that appears to be essential for mRNA maturation and transport [for reviews, see Dreyfuss (1986) and Merrill and Williams (1990)]. These six proteins have apparent molecular weights on SDS–PAGE that range from 32 000 to 44 000 and migrate as three doublets called, in order of increasing apparent molecular weight, A1/A2, B1/B2, and C1/C2 (Beyer et al., 1977). All 6 "core" hnRNP proteins contain 1 (type C) or 2 (type A or B) copies of an approximately 90 amino acid long region of extensive sequence homology that has been hypothesized to represent a conserved RNA binding motif (Dreyfuss et al., 1988; Merrill & Williams, 1990; Merrill et al., 1988; Query et al., 1989). Since this motif is found in a continuously enlarging group of eukaryotic proteins, including poly(A) binding protein (Sachs et al., 1986; Adam et al., 1986), the *Drosophila* sexual differentiation proteins sx1 (Bell et al., 1988) and tra-2 (Amrein et al., 1988; Goralski et al., 1989), and nucleolar proteins such as nucleolin (Lapeyere et al., 1987), among others, characterizing the interactions of hnRNP proteins with nucleic acids is of widespread interest. It seems reasonable to suppose that all these proteins that share this region of similarity will also be found to share at least part of their overall mechanism of binding.

Despite the fundamental role that hnRNP proteins are thought to play in hnRNA metabolism, very little data are available on their nucleic acid binding properties. What little data are available have frequently been obtained under nonequilibrium conditions (Schenkel et al., 1988; Swanson & Dreyfus, 1988a,b), sometimes relying on renaturation of SDS–polyacrylamide gel separated proteins (Schenkel et al., 1988), which may contribute to some apparent inconsistencies in the literature. Hence, while hnRNP particle reconstitution

† This work was supported in part by NIH Grant GM31539 to K.R.W.
‡ Yale University.
⊥ Present address: Bristol-Myers Squibb Co., Wallingford, CT 06492.
§ National Cancer Institute.
∥ Howard Hughes Medical Institute.

[1] Abbreviations: hnRNP, heterogeneous ribonucleoprotein; poly(ϵA), poly(ethenoadenylate); ω, cooperativity parameter.

0006-2960/91/0430-2968$02.50/0

studies fail to detect any sequence-specific binding by hnRNP proteins (LeStourgeon et al., 1990; Wilk et al., 1983; Pullman & Martin, 1983), an RNase protection study suggests specific high-affinity A1 and type C protein binding to the 3′ end of introns within a region containing the conserved poly(pyrimidine) stretch between the branch site and the 3′-splice site (Swanson & Dreyfuss, 1988a). Binding of A1 to an 18-nucleotide sequence within this region was found to be so specific that it was decreased greater than 10-fold by changing a single nucleotide (Swanson & Dreyfuss, 1988a). There is also disagreement in the literature over such a basic property as the ability of A1 hnRNP to bind double-stranded nucleic acids. Hence, while a nitrocellulose filter binding study (Kumar et al., 1986) found that A1 has equal affinity for single- and double-stranded nucleic acids, an SDS gel renaturation/blotting study (Swanson & Dreyfuss, 1988a) concluded that A1 cannot bind double-stranded nucleic acids. Similarly, whereas a nitrocellulose binding study (Kumar et al. 1986) found that A1 has equal affinities for poly(A), poly(C), and poly(U), a Sepharose binding study (Swanson & Dreyfuss, 1988b) concluded that A1 has considerably higher affinity for poly(U) as compared to either poly(C) or poly(A).

In order to resolve these apparent discrepancies, we have further characterized the equilibrium binding properties of A1 that has been overexpressed in *Escherichia coli* (Cobianchi et al., 1988). We have also carried out comparative studies on a limited cleavage fragment of A1 that contains residues 1–195 in this 34000-dalton protein (Kumar et al., 1986; Riva et al., 1986) and that has previously been isolated and studied as the UP1 helix-destabilizing protein (Herrick & Alberts, 1976). The 319-residue A1 protein (Cobianchi et al., 1988) contains two distinct domains that can be cleaved apart by limited trypsin digestion which preferentially occurs after arginine-195 (Kumar et al., 1986). The resulting NH_2-terminal fragment, UP1, contains two 92 amino acid long copies of the conserved eukaryotic RNA binding motif (Dreyfuss et al., 1988; Merrill & Williams, 1990; Merrill et al., 1988; Query et al., 1989). The COOH-terminal one-third of A1 has a quite different structure that bears no obvious sequence homology with the NH_2-terminal two-thirds and that has an unusually high, approximately 45%, glycine content (Cobianchi et al., 1988). By utilizing the protein-induced fluorescence enhancement of poly(ethenoadenylate), Cobianchi et al. (1988) found that the glycine-rich COOH-terminal domain contributes to A1 binding both through cooperative A1/A1 protein/protein interactions and through direct interaction with the nucleic acid. Hence, in 0.4 M NaCl, A1 binds with an affinity that is nearly 10^4-fold higher than that for UP1, and while A1 binds cooperatively, UP1 binds noncooperatively to this fluorescent polynucleotide analogue (Cobianchi et al., 1988).

Utilizing circular dichroism, thermal denaturation, and fluorescence spectroscopy, we have investigated the helix-destabilizing properties of A1 and UP1 as well as the relative affinities of these two proteins for RNA versus DNA and for single- versus double-stranded nucleic acids. Studies that will be described on the comparative salt sensitivity of A1 versus UP1 demonstrate that like the *E. coli* SSB ssDNA binding protein [see Lohman and Bujalowski (1990) for a review], the A1 occluded site size is highly dependent upon the salt concentration. The results of these studies provide an interesting parallel with previous studies on prokaryotic ssDNA binding proteins and provide a firm basis for further studies directed at understanding the functions of hnRNP proteins in mRNA maturation and transport.

Materials and Methods

Proteins and Nucleic Acids. A1 was purified as described in Cobianchi et al. (1988) except that the pH of all buffers was raised to 8. UP1 was obtained from A1 by proteolysis at 0 °C for 40 min with a 1:120 w/w ratio of trypsin. The reaction was stopped by adding 10 μL of diisopropyl fluorophosphate, diluted with 7 volumes of buffer A (50 mM Tris, pH 8.0, 1 mM EDTA, 1 mM DTT, and 10 mM $Na_2S_2O_5$) to lower the concentration of NaCl, and applied to a ssDNA–cellulose column equilbrated in buffer A containing 50 mM NaCl. UP1 was then eluted with a linear gradient to 1 M NaCl. All protein concentrations and amino acid compositions were determined on a Beckman System 7300 amino acid analyzer. Single- and double-stranded polynucleotides as well as the fluorescent polynucleotide analogue poly(ethenoadenylate) [poly(εA)] were from Pharmacia. Poly(dA) was ethenylated by incubation with 0.19 M chloroacetaldehyde in 20 mM sodium phosphate, pH 6.8, at 37 °C for 48 h as described by Kohwi-Shigematsu et al. (1978). The extent of the reaction was judged by the ratio of the absorbance of the modified polynucleotide at 260–320 nm according to the formula in Kohwi-Shigematsu et al. (1978) and was found to be complete. The following extinction coefficients in terms of nucleotide concentration were used: for poly(εA), $\epsilon_{257} = 3.7 \times 10^3$ M^{-1} cm^{-1} (Ledneva et al., 1978); poly(rA), $\epsilon_{257} = 1.03 \times 10^4$ M^{-1} cm^{-1}; poly(U), $\epsilon_{260} = 9.2 \times 10^3$ M^{-1} cm^{-1}; poly(dT), $\epsilon_{260} = 8.1 \times 10^3$ M^{-1} cm^{-1} (Overman et al., 1988); poly[d(A-T)], $\epsilon_{260} = 6.7 \times 10^3$ M^{-1} cm^{-1}; poly[r(A-U)], $\epsilon_{260} = 6.3 \times 10^3$ M^{-1} cm^{-1} (Giedroc et al., 1987).

Thermal Denaturation. The ability of A1 or UP1 to induce melting of either poly[d(A-T)] or poly[r(A-U)] was examined by monitoring the absorbance of these polynucleotides at 260 nm as a function of increasing temperature. A1 or UP1 plus the polynucleotide or the polynucleotide alone was dialyzed into buffer B (10 mM Tris, pH 8.0, 0.1 mM EDTA, and 0.1 mM DTT) containing 20 mM NaCl. The dialyzed mixtures were then placed in prechilled (10 °C) cuvettes in a Perkin Elmer Lambda 6 spectrophotometer equipped with a digital controller, temperature programmer, and thermoelectric cell holders. The temperature was increased to 77.5 °C at a rate of 1 °C/min.

Fluorescence Spectroscopy. Fluorescence titrations were performed on an SLM 8000C spectrofluorometer interfaced to an IBM XT computer. The average of three 10-s acquisitions was used for each data point. Forward titrations with poly(εA) and poly(dεA) were performed with an excitation wavelength of 315 nm and an emission wavelength of 400 nm. All fluorescence values were corrected for background fluorescence and for dilution effects due to addition of protein solutions to the cuvette. Reverse titrations with A1 or UP1 in the presence of poly(dT), poly(U), and poly(A) were performed with an excitation wavelength of 280 nm and an emission wavelength of 325 nm. Reverse titrations were corrected for background fluorescence, dilution, protein photobleaching, and inner filter effects due to the addition of polynucleotides. Inner filter corrections were derived from third-order regression of data obtained from titrating *N*-acetyltryptophanamide with the various polynucleotides.

Since our binding site size studies demonstrated that the maximum extent of poly[r(εA)] fluorescence enhancement at saturation decreases by 2–3-fold for A1 and by 2-fold for UP1 as the NaCl concentration is increased from 10 to 250 mM, it was not possible to use a single titration with subsequent salt additions to accurately determine the salt sensitivity of the binding of these proteins, as had been done previously by

Cobianchi et al. (1988). Therefore, separate titrations at each desired salt concentration were carried out, and the K_{app} for each curve was determined individually. Due to the tendency of A1 to precipitate in the absence of nucleic acid in NaCl concentrations below 500 mM, it was necessary to keep the concentrated protein stock solutions in either 400 mM NaCl (for the 25–200 mM NaCl titrations) or 800 mM NaCl (for the 300–400 mM NaCl titrations). Therefore, the salt concentration rose slightly (by 20–50 mM) during the titrations.

Determination of Binding Constants. As stated by Kowalczykowski et al. (1986), we could not determine K_{app} (equal to K_{int} times ω) at 50% saturation since for A1 and UP1 binding to nucleic acids the cooperativity parameter, ω, is not significantly greater than n. We therefore made use of the equation developed by McGhee and von Hippel (1974), which accounts for the presence of "gaps" and overlapping binding sites on the polynucleotide lattice. Using a fixed site size determined independently under stoichiometric conditions, we varied K_{int} and ω to obtain the best visual match of the theoretical curve [generated by using eq 15 of McGhee and von Hippel (1974)] to the experimental data. The procedure used is described by McSwiggen et al. (1988) and Kowalczykowski et al. (1986). Using this procedure, we were able to detect 2-fold differences in K_{int} or ω. We also made use of a log K_{app} versus log [NaCl] plot, termed a log–log plot. As described by Mascotti and Lohman (1990), the slope of the line from this plot divided by a thermodynamic constant yields an estimate of the maximum number of ionic interactions between protein and nucleic acid.

Circular Dichroism. Data for all circular dichroism experiments were collected on an Aviv circular dichroism spectropolarimeter Model 60DS over the range extending from 300 to 200 nm at 1-nm intervals, using a 1-cm path-length cuvette. The data from five repeat scans were used to fit the spectra as a polynomial function. The spectra of A1 or UP1 alone were subtracted from the spectra of polynucleotides with A1 and UP1 to correct for CD contributions from these proteins, although the CD spectra of A1 or UP1 indicate negligible contributions of protein circular dichroism above 240 nm.

Synthesis of the COOH-Terminal Peptide. The COOH-terminal peptide corresponding to residues 260–307 in A1 was synthesized at the Yale University School of Medicine Protein and Nucleic Acid Chemistry Facility using an Applied Biosystems 430A solid-phase peptide synthesizer. The yield of purified peptide from 0.2 mmol of resin was 34 mg by dry weight. Upon characterization by analytical HPLC, the purity was estimated to be greater than 95%. The observed amino acid analysis agrees quite well with the predicted analysis. The predicted protonated chemical molecular weight is 4911.2 which agrees well with the results of FAB mass spectroscopy which give a single positive ion isotopically unresolved peak at 4909.5.

Results

CD of Polynucleotides in the Presence of A1 or UP1. Previous physical studies on UP1 have shown that this protein suppressed both the positive and negative Cotton effects of poly(A) when the CD spectrum of this polynucleotide was obtained in the presence of increasing amounts of UP1 (Karpel & Burchard, 1980). These effects were interpreted as arising from unstacking of the polynucleotide bases upon protein binding. In contrast, Kumar et al. (1986) found no change in the CD spectrum of poly(A) upon adding the intact A1 protein that had been isolated from HeLa cells. We, however,

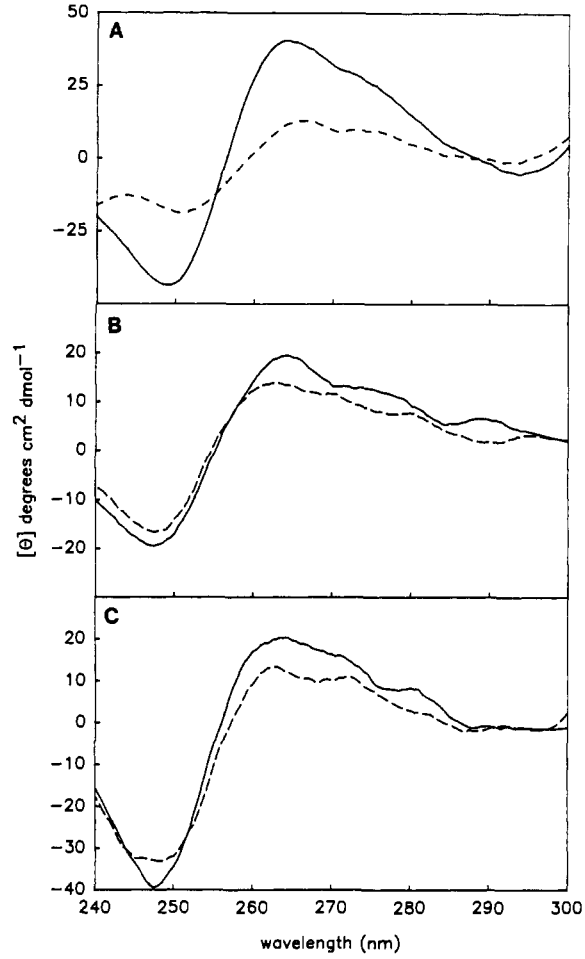

FIGURE 1: Circular dichroism of polynucleotides with and without A1 or UP1. The CD spectra of poly(A) and poly[d(A-T)] were taken in the absence (—) or presence (---) of stoichiometric amounts of A1 or UP1. The dashed lines are the spectra of the indicated polynucleotide and protein minus the spectrum of the protein alone. (A) 120 μM poly(A) with and without 10 μM A1. (B) 120 μM poly[d(A-T)] with and without 10 μM A1. (C) 70 μM poly[d(A-T)] with and without 10 μM UP1.

using A1 protein that had been overexpressed in *E. coli*, found that A1 strongly suppresses both the negative and positive Cotton effects of poly(A) (Figure 1A). This result is consistent with the fluorescence data of Cobianchi et al. (1988), which indicate that poly[r(ϵA)] is extensively unstacked upon binding A1. In agreement with Karpel and Burchard (1980), we found that UP1 also suppressed the positive and negative bands of the poly(A) spectrum (data not shown).

The addition of either A1 or UP1 also causes small changes in the spectrum of poly[d(A-T)] (Figure 1B,C). In both cases, there is a decrease in the positive band of the polynucleotide at 261 nm, which has been interpreted as being caused by the loss of double-helical structure in the case of the T4 gene 32 protein (Jensen et al., 1976). However, changes induced in the spectrum of poly[d(A-T)] by UP1 are somewhat more pronounced, and there is a shift in the wavelength minimum from 247.5 to 248.5 nm. This wavelength shift may indicate a helix–coil transition since it is also seen in thermal DNA denaturation with another protein (Greve et al., 1978). UP1 also caused an intense suppression of the positive band of poly[r(A-U)] but no shift in wavelength minimum (data not shown). Thus, from the CD data, it is apparent that while A1 binds strongly to poly(A), probably causing base unstacking, it is not clear whether or not it is functioning as a helix-destabilizing protein.

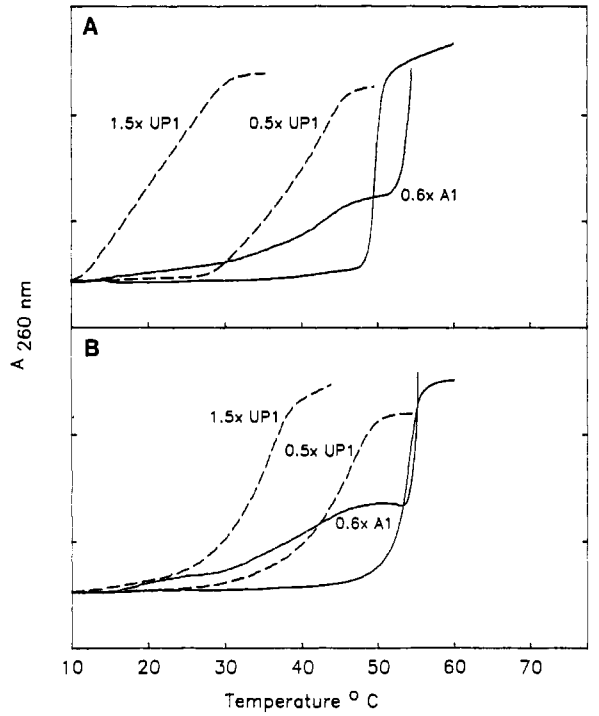

FIGURE 2: Thermal denaturation of poly[d(A-T)] or poly[r(A-U)] in the presence of A1 or UP1. All polynucleotides were at 30 μM in buffer B with 20 mM NaCl. The indicated equivalents of A1 or UP1 were added, assuming $n = 7$ for UP1 and $n = 14$ for A1. Each pair of ticks on the ordinate denotes 0.05OD unit. (A) Poly[d(A-T)] with and without A1 or UP1. (B) Poly[r(A-U)] with and without A1 or UP1. Since A1 denatures at about 50 °C, the apparent stabilization of double-stranded poly[d(A-T)] that occurs above 50 °C may result from an interaction between denatured A1 and double-stranded regions in poly[d(A-T)]. This unusual phenomenon is less apparent in the case of the more stable poly[r(A-U)].

Thermal Denaturation of Poly(rA-rU) and Poly(dA-dT) in the Presence of A1 or UP1. UP1 has previously been shown to destabilize the partially double-stranded polynucleotide poly[d(A-T)] (Herrick & Alberts, 1976). In contrast, the decreased ability of A1 as compared to UP1 to stimulate DNA polymerase α activity in vitro has been hypothesized to result from a postulated inability of the intact A1 protein to destabilize double-stranded nucleic acids (Riva et al., 1986).

We directly tested the ability of A1 and UP1 to destabilize partially double-stranded poly[r(A-U)] and poly[(A-T)] helices. When a small excess of A1 to polynucleotide was present (1.2:1 based on $n = 14$, see below), no helix destabilization was observed before the onset of protein denaturation, which occurred at approximately 45–50 °C (data not shown). In contrast a 1.5:1 excess of UP1 to polynucleotide (assuming $n = 7$) resulted in lowering the apparent T_m for poly[d(A-T)] by 30 °C, and that for poly[r(A-U)] by 20 °C (Figure 2A,B). However, when a substoichiometric amount of A1 was used (A1:polynucleotide binding site ratio of 0.6:1), both RNA and DNA duplexes were destabilized, and there was a clear distinction between the effect of a substoichiometric amount of UP1 vs A1. That is, based on the final extent of hyperchromicity, it appears that 50% saturation with UP1 is sufficient to depress the T_m of virtually 100% of the poly[r(A-U)] present by 10 °C (see Figure 2B). In contrast, on the basis of the final extent of hyperchromicity reached, 60% saturation with A1 appears to descrease the T_m of only 40% of the poly[r(A-U)] present by about 13 °C.

Binding of A1 and UP1 to Double-Stranded DNA. The melting data suggest that native A1 and UP1 have higher affinities for single-stranded as compared to double-stranded

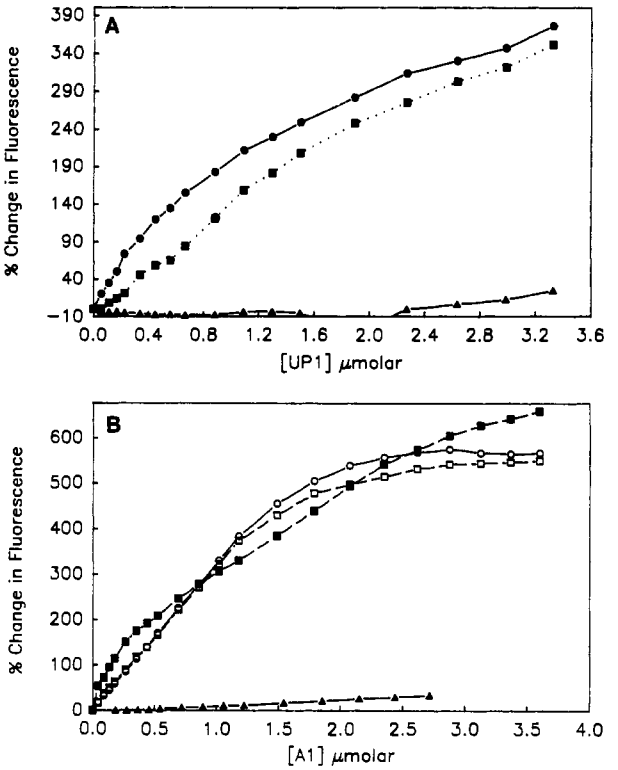

FIGURE 3: Fluorescence titrations of poly[d(ϵA)] with UP1 or A1 in the presence of excess ϕX174 ssDNA or ϕX174 dsDNA (relaxed form). (A) Poly[d(ϵA)] (1 μM) in buffer B with 25 mM NaCl was titrated with UP1: poly[d(ϵA)] only (filled circles); poly[d(ϵA)] + 100 μM ϕX174 single-stranded DNA (filled triangles); poly[d(ϵA)] + 100 μM ϕX174 double-stranded DNA (filled squares). (B) Poly[d(ϵA)] (1 μM) in buffer B with 150 mM NaCl was titrated with A1: poly[d(ϵA)] only (open circles); poly[d(ϵA)] + 100 μM (phosphate) ϕX174 virion ssDNA (filled triangles); poly[d(ϵA)] + 10 μM ϕX174 double-stranded DNA (open squares); poly[d(ϵA)] + 100 μM ϕX174 double-stranded DNA (filled squares). Since the curves for UP1 and for A1 + 100 μM ϕX174 double-stranded DNA indicate saturation was not reached, an extrapolated value at saturation of 380% for UP1 and 682% for A1 based on these curves plus other titrations carried out under similar conditions was used to estimate K_{app}.

nucleic acids. To test this idea further under equilibrium conditions, we utilized competition assays, where the binding of A1 and UP1 to poly[d(ϵA)] under nonstoichiometric conditions was competed for by the presence of either the single-stranded virion form or the nicked (relaxed) double-stranded form of ϕX174 DNA. As can be seen in Figure 3A,B, the presence of a 100-fold excess of the single-stranded form of ϕX DNA almost completely eliminated the binding of UP1 and of A1 to poly[d(ϵ-A)], as evidenced by the lack of fluorescence enhancement of the poly[d(ϵA)] upon addition of UP1 or A1. In contrast, the addition of a 100-fold molar excess of double-stranded ϕX174 DNA to UP1 resulted in only a modest reduction in the apparent affinity of UP1 for poly[d(ϵA)]. On the basis of the assumption that the free protein concentration is the same at a similar percentage of fluorescence enhancement (with or without competitor DNA present), we calculated a binding constant for ϕX174 DNA. We estimate the K_{app} for UP1 binding to single- and double-stranded ϕX174 as 1.1×10^6 and 3.1×10^3 M^{-1}, respectively. Therefore, UP1 has an approximately 350-fold higher affinity for single- versus double-stranded DNA. As shown in Figure 3B, the presence of a 10-fold molar excess of double-stranded ϕX174 DNA results in a titration curve with A1 that is nearly identical with the titration of poly[d(ϵA)] alone. The K_{app} for the titration with a 10-fold excess of double-stranded DNA

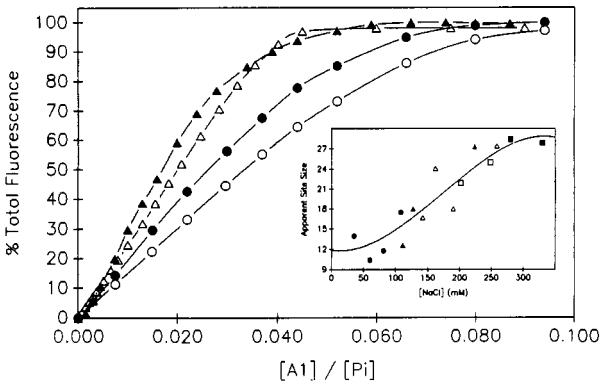

FIGURE 4: Effect of NaCl concentration on the occluded site size of A1 binding to the poly[r(ϵA)]. Forward titrations of 1 μM poly[r(ϵA)] with A1 at the indicated NaCl concentration were performed under stoichiometric conditions. The NaCl concentrations are as follows: (open circles) 25 mM; (closed circles) 100 mM; (open triangles) 150 mM; (closed triangles) 200 mM. Inset: Plot of the apparent occluded site size versus NaCl concentration. The NaCl concentration indicated is the concentration at the stoichiometric point of each titration. Each data point in the inset represents a titration of A1 with the following concentrations of poly[r(ϵA)]: (closed circles) 1 μM r(ϵA); (open triangles) 2 μM r(ϵA); (closed triangles) 5 μM r(ϵA); (open squares) 10 μM r(ϵA); (closed squares) 20 μM r(ϵA).

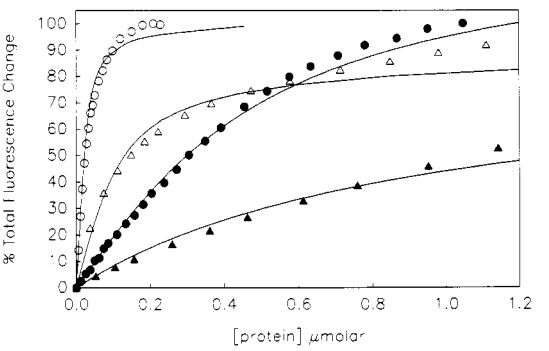

FIGURE 5: Fluorescence titrations of poly[r(ϵA)] and poly[d(ϵA)] with A1 or UP1. Starting polynucleotide concentrations were 1 μM phosphate. Titrations were carried out in buffer B containing 25 mM NaCl for the UP1 titrations and in buffer B containing 200 mM NaCl for the A1 titrations. The solid lines are theoretical best-fit curves generated as described under Material and Methods. A1 and poly[r(ϵA)], open circles; A1 and poly[d(ϵA)], filled circles; UP1 and poly(ϵA), open triangles; UP1 and poly[d(ϵA)], filled triangles.

was 1.1×10^6 M^{-1}, virtually identical with a K_{app} of 1.0×10^6 M^{-1} for the poly[d(ϵA)] curve alone. Because of the unusual shape of the A1 poly[d(ϵA)] titration curve in the presence of a 100-fold excess of ds DNA, we have not attempted to calculate an affinity constant for these data. It is obvious, however, from the data in Figure 3B that ssDNA competes considerably better than dsDNA does for binding to A1.

Fluorescence Binding Studies of A1 and UP1 to ssRNA versus ssDNA as a Function of Salt Concentration. During our initial studies on the influence of salt concentration on A1 binding to poly[r(ϵA)], we found that as the NaCl concentration was increased, the nucleic acid lattice was saturated at much lower protein concentrations. We therefore performed titrations of A1 with poly[r(ϵA)] under stoichiometric conditions at varying salt concentrations. As seen in Figure 4, as the NaCl concentration was increased, saturation was reached at lower protein concentrations, indicating an apparent increase in the occluded site size. When several titrations were carried out at varying salt and poly[r(ϵA)] concentrations, all under stoichiometric conditions, the relationship shown in Figure 4 (inset) was seen between the site size and the [NaCl]. There appears to be an increase in the site size by a factor of 2 as the NaCl concentration is increased over the range extending from 25 to 250 mM. (At any given NaCl concentration, there was typically no greater than 10% variation in the site size, *n*.) This phenomenon is independent of the initial poly[r(ϵA)] concentration. To eliminate the possibility that A1 precipitation might be causing the apparent change in site size, which appears unlikely since A1 appears to precipitate more at low rather than high salt, the A1 protein concentration was determined by hydrolysis and amino acid analysis of aliquots taken from A1/poly[r(ϵA)] titrations carried out at two different salt concentrations. We obtained nearly identical protein concentrations in 25 versus 200 mM NaCl, suggesting there was no salt-dependent precipitation phenomenon. Due to our inability to obtain stoichiometric binding of A1 versus poly[d(ϵA)] and UP1 versus poly[r(ϵA)] or poly[d(ϵA)] in high salt, we were unable to determine whether there is a similar site size change for UP1 or for A1 with poly[d(ϵA)]. Titrations of UP1 with 1–10 μM poly[r(ϵA)] in 10 mM NaCl were stoichiometric as evidenced by obtaining an identical site size of 8 over a 10-fold range in the initial poly[r(ϵA)] concentration. Stoichiometric titrations of A1 with poly[d(ϵA)] in 25 mM NaCl yielded a site size of 14, similar to the site size with poly[r(ϵA)]. In order to calculate binding affinities, we made the assumption that the A1 site size is equivalent for both poly[r(ϵA)] and poly[d(ϵA)] and that the UP1 site size does not vary with the NaCl concentration and is the same for RNA as well as DNA.

As can be seen in Figure 5, both for A1 and UP1 there was a significant difference in binding to DNA versus RNA which results from differences in the intrinsic affinity as opposed to the cooperativity of binding of these proteins to nucleic acids. Over a wide range of NaCl concentrations (25–400 mM), the cooperativity parameter, ω, for A1 binding to either RNA or DNA was 35 ± 32 (mean ± SD). These data are in good agreement with the value of 30 which was obtained by Cobianchi et al. (1988) in 400 mM NaCl, and indicate there is no significant dependence of ω on salt concentration. In 200 mM NaCl, the K_{app} was $\geq 2.9 \times 10^8$ M^{-1} for A1 binding to poly[r(ϵA)] and 1.7×10^6 M^{-1} for A1 binding to poly[d(ϵA)]. Therefore, in 200 mM NaCl, the apparent affinity of A1 is at least 170-fold stronger for RNA than for DNA. UP1 also has a higher affinity for RNA than for DNA. The best-fit plots of data for 1 μM poly[r(ϵA)] versus UP1 in 10 mM NaCl yielded $K_{app} = 2.8 \times 10^7$ M^{-1} and for UP1 versus poly[d(ϵA)], $K_{app} = 2.6 \times 10^6$ M^{-1}. The cooperativity parameter was 1–2, indicative of a lack of cooperativity for UP1 binding to polynucleotides. As discussed by Takahashi et al. (1989), the oligomerization state of the protein has an effect upon the cooperativity parameter determined by using the equations of McGhee and von Hippel (1974). If A1 was in fact a dimer, whereas we have assumed a monomer, then our determination of ω would be a 2-fold underestimate.

The data from a series of titrations at different NaCl concentrations are summarized in Table I. Again, it is obvious that A1 binds stronger to RNA than to DNA. Interestingly, it appears that there is more specificity for RNA at low salt than at high salt concentrations. When a log K_{app} versus log [NaCl] plot is used of the data in Table I, A1 should have an approximately equal affinity for RNA and DNA at about 0.48 M NaCl. Since binding is extremely strong for A1 to poly[r(ϵA)] below 150 mM NaCl, and appears to be at the limit of detection for the fluorescence titrations, we were unable to directly determine a binding constant at very low salt. However, when the data from a log–log plot are extrapolated to 25 mM NaCl, there is a (1×10^5)-fold preference for A1 binding to RNA than DNA, whereas at 400 mM salt there

Table I: Summary of A1, UP1, and C-Terminal Peptide Binding to Poly[r(ϵA)] and Poly[d(ϵA)] at Various Salt Concentrations[a]

protein	starting [NaCl] (mM)	poly[r(ϵA)] K_{app} (M^{-1})	poly[d(ϵA)] K_{app} (M^{-1})	N^b
A1	25		1.5×10^7	14
	100		1.0×10^7	18
	150	2.7×10^8	3.9×10^6	21
	200	2.9×10^8	1.7×10^6	26
	300	1.2×10^7	4.8×10^6	28
	325	1.5×10^7		28
	350	6.5×10^6	2.7×10^6	28
	375	6.6×10^6		28
	400	6.3×10^6	2.2×10^6	28
UP1	10	2.8×10^7	2.6×10^6	8
	25	3.5×10^6		8
	50	1.6×10^6		8
	75	1.5×10^5		8
	100	6.0×10^4		8
	130	5.0×10^4		8
COOH-terminal peptide	5	3.6×10^6		3
	10	1.5×10^6	2.3×10^5	3
	15	5.6×10^5		3
	20	5.8×10^5		3
	25	5.2×10^5		3

[a] All calculations were based on curve fitting using the procedures described under Materials and Methods. For those salt concentrations where it was possible to determine a cooperativity parameter, ω, it was found to vary randomly with salt concentration. The cooperativity parameter over the entire range of salt concentrations was 30 ± 31, 43 ± 32, and 27 ± 27 for A1/poly[r(ϵA)], A1/poly[d(ϵA)], and COOH-terminal peptide/poly[r(ϵA)], respectively. UP1 binding to poly[r(ϵA)] or poly[d(ϵA)] was essentially noncooperative with ω = 1–2. [b] The occluded site sizes sites reported in this table for A1 are the assumed values based on the data in Figure 4. Each value is the mean of at least two determinations. The linear least-squares lines of the log–log plots are as follows: A1 + poly(ϵA), slope (m) = 4.6, y_{int} = 4.9; A1 + poly[d(ϵA)], m = 0.7, y_{int} = 6.0; UP1/poly(ϵA), m = 2.9, y_{int} = 2.0.

is only a 3-fold difference. These data would suggest that A1 binding to RNA involves electrostatic interactions which are not available when A1 binds to DNA.

Finally, as seen in Table I, UP1 binds approximately 10-fold stronger to RNA than to DNA in 10 mM NaCl. In contrast, when the binding of A1 is extrapolated to 10 mM NaCl, there is an approximately (3×10^6)-fold specificity for RNA versus DNA. This suggests that at least at low NaCl concentrations, the glycine-rich, COOH terminus of A1 contributes greater than 80% of the preferential free energy of binding for RNA versus DNA.

Binding of a COOH-Terminal Synthetic Peptide Analogue of A1 to RNA and DNA. On the basis of the comparative binding properties of A1 and UP1, we have inferred that the COOH terminus of A1 plays an important role in binding to nucleic acids. In an attempt to directly determine the binding characteristics of this COOH-terminal domain, we have synthesized a peptide as described under Materials and Methods which corresponds to residues 260–307 of the A1 protein. This peptide represents approximately 40% of the C-terminal domain. The sequence of the peptide is as follows: N-D-F-G-N-Y-N-N-Q-S-S-N-F-G-P-M-L-G-G-N-F-G-G-R-S-S-G-P-Y-G-G-G-G-Q-Y-F-A-L-P-R-N-Q-G-G-Y-Y-G-G-S. This peptide is different from the peptide studied by Cobianchi et al. (1988) which consisted of an oligomerized 16-residue repeating sequence.

We have characterized some of the nucleic acid binding properties of this 48-residue peptide. Table I summarizes data from titrations of the COOH-terminal peptide with poly[r(ϵA)] and poly[d(ϵA)] at various salt concentrations. There appears to be only a slight salt dependence of binding. As

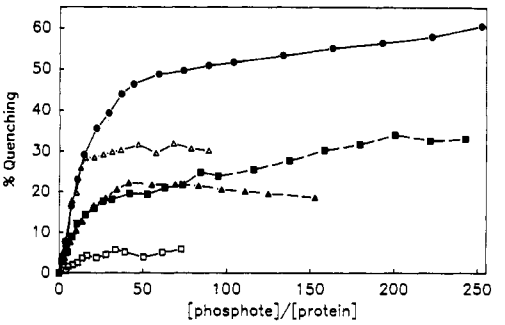

FIGURE 6: Reverse titrations of A1 and UP1 with homopolynucleotides. Solutions of A1 in buffer B/200 mM NaCl were titrated by additions of either poly(U) (filled triangles), poly(A) (filled squares), or poly(dT) (filled circles). Solutions of UP1, 2.4 μM in buffer B/50 mM NaCl, were titrated with either poly(U) (open triangles) or poly(A) (open squares).

expected, the slope of the log–log plot of these data of approximately 1 is close to the corresponding difference in the slopes of the A1 versus UP1 log–log plots, which is equal to about 1.7. It is clear from the data in Table I that this peptide binds approximately 7-fold tighter to RNA than to DNA. Finally, curve fitting these data yields a cooperativity parameter, ω, of 27 ± 27 (mean ± SD). This is in the range of ω which was determined for the A1 protein and suggests that all A1/A1 cooperative protein/protein interactions may be mediated via interactions occurring within the glycine-rich, COOH-terminal domain.

Reverse Titrations of A1 and UP1. All of the fluorescence experiments described so far have relied on the fluorescence enhancement of polynucleotide analogues that is induced by protein binding. The limitation of this technique is that it is restricted to the poly(ϵA) and poly[d(ϵA)] derivatives. In order to directly determine the differential affinity of A1 and UP1 for various polynucleotides, we monitored the quenching of the intrinsic protein fluorescence that results from the binding of polynucleotides. When an excitation wavelength of 280 nm and an emission wavelength of 325 nm are used, titrations of A1 and UP1 with either poly(A), poly(U), or poly(dT) result in substantial quenching of the intrinsic protein fluorescence, particularly in the case of A1 titrated with poly(dT), where approximately 70% quenching is observed (Figure 6). Due to the tendency of A1 to precipitate in low salt in the absence of polynucleotide, it was not possible to obtain curves for A1 under stoichiometric conditions. It was, however, possible to obtain comparisons of a few polynucleotides under similar conditions. The K_{app} values for the titration curves shown in Figure 6 suggest that there is not a substantial degree of base specificity in A1 binding; that is, in 200 mM NaCl, the K_{app} for A1 binding to poly(U) is 2.0×10^6 M^{-1} compared to 3.2×10^5 M^{-1} for poly(A). This 6-fold difference, which is in qualitative agreement with the previous Sepharose binding assays of Swanson and Dreyfuss (1988b), probably results from the fact that while poly(U) lacks any significant secondary structure in solution at room temperature, poly(A) is highly base-stacked (Saenger, 1984). Hence, the apparent differences in affinity for these two polynucleotides may merely reflect the free energy that is required to disrupt the preexisting base stacking of poly(A) prior to A1 binding. The comparatively high affinity A1 has for poly(dT) (1.1×10^6 M^{-1}), only 2-fold less than that for poly(U), is also probably due to the fact that poly(dT) in solution has little secondary structure (Saenger, 1984). The K_{app} for the A1 vs poly(dT) titration is only an estimate since, as is apparent in Figure 6, saturation has not been reached. The biphasic shape of the curve may result from the change in A1 binding modes from cooperative

to noncooperative caused by a decrease in free A1 concentration as the titration progresses, as is discussed in Kowalczykowski et al. (1986). We were unable to obtain successful titrations without protein precipitation for poly(G) and poly(C). UP1 also had a very slight base specificity. On the basis of the data in Figure 6, UP1 bound to poly(U) with a K_a of 4.7×10^5 M^{-1} and to poly(A) with a binding constant of 1.4×10^6 M^{-1}.

A comparison of the poly(A) data in Figure 6 to the poly(εA) data in Table I suggests that A1 binds about 900-fold more tightly to poly(εA), since the K_{app} for the A1/poly(εA) complex in 200 mM NaCl is 2.9×10^8 M^{-1}, while the K_{app} for the A1/poly(A) complex in 200 mM NaCl is only 3.2×10^5 M^{-1}. This phenomenon has been observed in titrations of T4 gene 32 protein with poly(A) and poly(εA), where the K_{app} for poly(εA) was approximately 40-fold higher than the K_{app} for poly(A) (Newport et al., 1981).

Discussion

Fluorescence titration data obtained with poly(εA) and CD data obtained with poly(A) both suggest that binding of A1 and UP1 both result in a similar unstacking of the nucleic acid bases. Since A1 binds nucleic acids with a cooperativity parameter of about 35, while UP1 binds noncooperatively, unstacking of the nucleic acid bases is apparently not dependent on the formation of long stretches of contiguously bound protein. Both A1 and UP1 have higher affinities for single-stranded versus double-stranded polynucleotides, and thus, as expected, both act as helix-destabilizing proteins. The T_m depression for both A1 and UP1 is slightly greater for poly[d(A-T)] than for poly[r(A-U)], which may only reflect the fact that under similar conditions, the melting temperature of poly[r(A-U)] is somewhat higher, and hence partially double-stranded poly[r(A-U)] is more stable than partially double-stranded poly[d(A-T)] (Herrick & Alberts, 1976).

Despite the fact that both A1 and UP1 are helix-destabilizing proteins, there are differences in the effect of these two proteins on the thermal denaturation of partially double-stranded polynucleotides. That 0.5 equiv of UP1 causes a shift in the melting temperature of almost all of the poly[r(A-U)] present, while 0.6 equiv of A1 causes premelting of only 40% of the polynucleotide present, can be rationalized by the fact that A1, which binds cooperatively, will bind poly[r(A-U)] in long contiguous stretches, thus leaving much of the poly[r(A-U)] unliganded. In contrast, the noncooperatively binding UP1 should bind in a more distributive fashion and thus even at 50% saturation is able to influence the T_m of nearly 100% of the poly[r(A-U)] present. Some degree of helix-destabilizing activity could be imagined to play a role in the processing of pre-mRNA, perhaps by melting out undesired secondary structure to allow the RNA "template" to interact with the splicing machinery. Surprisingly, when A1 is present in stoichiometric amounts, no helix-destabilizing activity is observed prior to protein denaturation. This phenomenon is not simply dependent upon the A1 concentration, since doubling the concentration of polynucleotide (from 2.5 to 5 μM by site size) while keeping the A1 concentration constant at 2.9 μM does result in premelting of some of the poly[r(A-U)] (data not shown). Thus, it may be that the A1/polynucleotide complex itself has limited solubility, and saturating amounts of A1 (at the concentrations required for the melting experiments) may exceed the solubility limit of the complex. Given the tendency of A1 to form a trimer in an hnRNP particle and to precipitate in low-salt buffers, a competing A1/A1 protein interaction that might occur between A1 molecules that either are free in solution or are bound to a nucleic acid lattice also cannot be ruled out. In either case, the glycine-rich COOH terminus of A1 appears to be responsible for the observed phenomenon.

We have shown that the site size for A1 binding to RNA is dependent on NaCl concentration. A salt-dependent change in site size has also previously been shown to occur for the tetrameric *E. coli* SSB protein. The site size of the SSB–polynucleotide complex increases from about 35 to 65 as the salt concentration is increased from about 10 mM to above 200 mM NaCl (Lohman & Overman, 1985). These two SSB binding modes have been proposed to be topologically distinct in that in the $n = 35$ mode only two monomers within a SSB tetramer are thought to be in contact with the nucleic acid. In contrast, in the $n = 65$ mode, each of the four monomers in a SSB tetramer have been proposed to contact the nucleic acid. In the case of A1, we found that like SSB, the occluded site size also doubles over this same range of salt concentrations. That is, the occluded site size for A1 increases from about 12–14 in 25 mM NaCl to about 27–28 in 250 mM NaCl.

Both A1 and UP1 bind preferentially to RNA over DNA. The differences in affinities are much greater for A1 than for UP1, particularly in NaCl concentrations below 200 mM. For example, at 10 mM NaCl, the affinity of UP1 for poly[r(εA)] is only 11-fold greater than the affinity of UP1 for poly[d(εA)]. In contrast, the value for K_{app} for A1 binding to poly[r(εA)] in 10 mM NaCl, extrapolated from the log–log plots in Figure 6, is 1.0×10^{14} M^{-1}. This is (3×10^6)-fold greater than the value of A1 binding to poly[d(εA)] under the same conditions. There is only a fewfold difference in the affinities of UP1 and A1 for RNA versus DNA at higher salt concentrations. This suggests that at least some of the additional interactions involved in the ability of A1 to discriminate between RNA and DNA are electrostatic in nature. The slopes of the log–log plots of the data in Table I should correlate with the number of ionic interactions that can occur between A1 and the nucleic acid lattice. A1 binding to RNA yields a slope of 4.5 compared to A1 binding to DNA which has a slope of only 0.7. The slope of the UP1/RNA log–log plot is approximately 3. These results differ from those previously reported by Cobianchi et al. (1988), who found that UP1 binding to RNA was more salt sensitive than A1 binding to RNA. However, Cobianchi et al. (1988) used only one titration with subsequent salt additions which could yield erroneous results due to the failure of this approach to correct for variation in the final extent of maximum fluorescence enhancement with respect to NaCl concentration. In support of this notion, we performed a titration of A1 using the procedure described by Cobianchi et al. (1988) and obtained a slope in the log–log plot which was similar to the slope reported in their study (data not shown).

The results described above suggest that the differences in K_{app} between A1 and UP1 are not due to differences in ω alone. For example, in 25 mM NaCl, K_{app} of A1 for poly[r(εA)] is 1.5×10^{12} M^{-1}, a minimum estimate from the log–log plot in Figure 6, while K_{app} for UP1 is 3.5×10^6 M^{-1}, approximately (4×10^5)-fold less. Since ω values for UP1 are 1 or 2 (see Table I) compared to an ω value of about 30 for A1, this difference would only account for a 30-fold difference in K_{app}. The additional binding energy of A1 therefore must come from additional interactions between the A1 COOH-terminal region and poly[r(εA)]. This result has been further substantiated by studies carried out on a COOH-terminal synthetic peptide corresponding to residues 260–307. This peptide binds to nucleic acids with a cooperativity parameter

that is nearly identical with that for A1. Therefore, these cooperative interactions may account for the full cooperativity of A1, indicating the COOH terminus of A1 is directly involved in protein/protein interactions. Since the A1 cooperativity parameter appears to be insensitive to the NaCl concentration, these cooperative protein/protein interactions are probably not dependent upon ionic interactions. As expected from comparative binding studies on A1 versus UP1, the COOH-terminal peptide also has a relatively high intrinsic affinity for poly[r(ϵA)]. In 100 mM NaCl, this peptide binds to poly[r(ϵA)] with an overall affinity of 7×10^4 M^{-1}, as estimated from the log–log plot. Under the same conditions, UP1 binds with a K_{app} of 6×10^4 M^{-1}, and A1 binds with an estimated K_{app} of 3×10^9 M^{-1}. Therefore, the sum of the free energy of binding of UP1 and of the COOH-terminal peptide is essentially equivalent to the overall binding energy of A1. In fact, over the entire salt concentration range extending from 10 to 400 mM NaCl, both the amino-terminal portion of A1 and also the COOH-terminal domain appear to contribute approximately equally and independently to RNA binding. The COOH-terminal region does not seem to contribute significant base specificity of binding, since K_{app} values of A1 or UP1 with poly(A), poly(U), or poly[d(T)] are similar, within an order of magnitude of each other. The helix-destabilizing activity of A1 is also not enhanced by the presence of the glycine-rich COOH terminus. Contrary to the emphasis that has been placed on the presence of two eukaryotic RNA binding motifs within the UP1 portion of A1 (Dreyfuss et al., 1988; Merrill & Williams, 1990; Merrill et al., 1988; Query et al., 1989), our studies indicate that the protein/protein and protein/nucleic acid interactions contributed by the glycine-rich COOH-terminal portion of A1 account for half of the overall free energy of A1 binding to a long single-stranded nucleic acid lattice. It is important to mention that it is thought that the A1 hnRNP protein functions in vivo as part of a 40S hnRNP complex (LeSturgeon et al., 1990). Therefore, the binding properties of A1 with nucleic acids may be significantly altered when this protein is part of this large complex.

Acknowledgments

We thank Ernest Hill for writing the fluorescence titration and analyis programs and Joseph Shiloach for growing large-scale cultures of cells containing the A1 overexpression vector. We also thank James Elliott of the Yale University School of Medicine Protein and Nucleic Acid Chemistry Facility for preparing the COOH-terminal peptide and Walter McMurray from the Yale University Comprehensive Cancer Center Mass Spectrometry Facility for the mass spectral analysis. We also thank Katy Schrader for typing the manuscript.

References

Adam, S. A., Nakagawa, T., Swanson, M. S., Woodruff, T. K., & Dreyfuss, G. (1986) *Mol. Cell. Biol. 6*, 2932–2943.

Amrein, H., Gorman, M., & Nöthiger, R. (1988) *Cell 55*, 1025–1035.

Bell, L. R., Maine, E. M., Schedl, P., & Clone, T. W. (1988) *Cell 55*, 1037–1046.

Beyer, A. L., Christensen, M. E., Walker, B. W., & LeStourgeon, W. M. (1977) *Cell 11*, 127–138.

Bujalowski, W., Overman, L. B., & Lohman, T. M. (1988) *J. Biol. Chem. 263*, 4629–4640.

Cobianchi, F., Karpel, R. L., Williams, K. R., Notario, V., & Wilson, S. H. (1988) *J. Biol. Chem. 263*, 1063–1071.

Dreyfuss, G., Swanson, M. S., & Pinol-Roma, S. (1988) *Trends Biochem. Sci. (Pers. Ed.) 13*, 86–91.

Giedroc, D. P., Keating, K. M., Williams, K. R., & Coleman, J. E. (1987) *Biochemistry 26*, 5251–5259.

Goralski, T. J., Edstrom, J. E., & Baker, B. J. (1989) *Cell 56*, 1011–1018.

Greve, J., Maestre, M. F., Moise, H., & Hosoda, J. (1978) *Biochemistry 17*, 893–898.

Herrick, G., & Alberts, B. (1976) *J. Biol. Chem. 251*, 2133–2141.

Jensen, D. E., Kelley, R. C., & von Hippel, P. H. (1976) *J. Biol. Chem. 251*, 7215–7228.

Karpel, R. L., & Burchard, A. C. (1980) *Biochemistry 19*, 4674–4682.

Karpel, R. L., Miller, N. S., & Fresco, J. R. (1982) *Biochemistry 21*, 2102–2108.

Kohwi-Shigematsu, T., Enomoto, T., Yamada, M. A., Nakanishi, M., & Tsuboi, M. (1978) *Proc. Natl. Acad. Sci. U.S.A. 75*, 4689–4693.

Kowalczykowski, S. C., Paul, L. S., Lonberg, N., Newport, J. W., McSwiggen, J. A., & von Hippel, P. H. (1986) *Biochemistry 25*, 1226–1240.

Kumar, A., Williams, K. R., & Szer, W. (1986) *J. Biol. Chem. 261*, 11266–11273.

Ledneva, R. K., Razjivin, A. P., Kost, A. A., & Bogdanov, A. A. (1978) *Nucleic Acids Res. 5*, 4225–4243.

LeStourgeon, W. M., Barnett, S. F., & Northington, S. J. (1990) in *The Eukaryotic Nucleus: Molecular Biochemistry and Macromolecular Assemblies* (Strauss, P., & Wilson, S., Eds.) Vol. 2, pp 477–502, Telford Press, London.

Lohman, T. M., & Overman, L. B. (1985) *J. Biol. Chem. 260*, 3594–3603.

Lohman, T. M., & Bujalowski, W. (1990) in *The Biology of Nonspecific DNA–Protein Interactions* (Revzin, A., Ed.) CRC Press, Boca Raton, FL (in press).

Mascotti, D. P., & Lohman, T. M. (1990) *Proc. Natl. Acad. Sci. U.S.A. 87*, 3142–3146.

McGhee, J. D., & von Hippel, P. H. (1974) *J. Mol. Biol. 86*, 469–489.

McSwiggen, J. A., Bear, D. G., & von Hippel, P. H. (1988) *J. Mol. Biol. 199*, 609–622.

Merrill, B. M., & Williams, K. R. (1990) in *The Eukaryotic Nucleus: Molecular Biochemistry and Macromolecular Assemblies* (Strauss, P., & Wilson, S., Eds.) Vol. 2, pp 579–604, Telford Press, London.

Merrill, B. M., Stone, K. L., Cobianchi, F., Wilson, S. H., & Williams, K. R. (1988) *J. Biol. Chem. 263*, 3307–3313.

Newport, J. W., Lonberg, N., Kowalczykowski, S. C., & von Hippel, P. H. (1981) *J. Mol. Biol. 145*, 105–121.

Overman, L. B., Bujalowski, W., & Lohman, T. M. (1988) *Biochemistry 27*, 456–471.

Pullman, J. M., & Martin, T. F. (1983) *J. Cell Biol. 97*, 99–111.

Query, C. C., Bentley, R. C., & Keene, J. D. (1989) *Cell 57*, 89–101.

Riva, S., Morandi, C., Pandolfo, M., Biamonti, G., Merrill, B., Williams, K. R., Multhaup, G., Beyreuther, K., Werr, H., Henrich, B., & Schafer, K. P. (1986) *EMBO J. 5*, 2267–2273.

Sachs, A. B., Bond, M. W., & Kornberg, R. D. (1986) *Cell 45*, 827–835.

Saenger, W. (1984) *Principles of Nucleic Acid Structure*, Springer-Verlag, New York.

Schenkel, J., Sekeris, C., Alonso, A., & Bautz, E. K. E. (1988) *J. Biochem. 171*, 565–569.
Swanson, M. S., & Dreyfuss, G. (1988a) *EMBO J. 7*, 3519–3529.
Swanson, M. S., & Dreyfuss, G. (1988b) *Mol. Cell. Biol. 8*, 2237–2241.
Wilk, H., Angeli, G., & Shafer, K. (1983) *Biochemistry 22*, 4592–4600.

Design of a Helix-Bundle Cross-Link: NMR and UV–Visible Spectroscopic Analyses and Molecular Modeling of Ring-Oxidized Retinals

Thomas C. Williams*,‡ and Venkatachalam Mani§

Departments of Pharmacology and Ophthalmology, Medical University of South Carolina, Charleston, South Carolina 29425-2251, and M&S Data Analysis and Molecular Speculations, Charleston, South Carolina 29417

Received July 19, 1990; Revised Manuscript Received December 17, 1990

ABSTRACT: In order to generate potential chemical cross-links for studying the chromophore binding site of bacteriorhodopsin and related helix-bundle proteins, MnO_2 was used to oxidize *all-trans*-retinal's ring moiety. The structures and solution conformations of three ring-oxidized retinal analogues have been determined by using UV–visible absorption and ^1H and ^{13}C NMR spectroscopies, primarily with regard to (i) the introduction of a functional group at the ring end of the chromophore, (ii) the retention of the all-trans geometry of the polyenal side chain, and (iii) the torsional angle of the ring–polyenal bond. Analyses of their UV–visible absorption spectral parameters (λ_{max}, ϵ_{max}, and vibrational fine structure) and NMR spectral parameters (^1H–^1H coupling constants, ^1H and ^{13}C NMR chemical shifts, and ^1H homonuclear Overhauser effects) indicated the 4-oxo and the 2,3-dehydro-4-oxo derivatives both possess the twisted 6-s-cis conformation adopted by most six-membered ring analogues of retinal in solution or crystal. However, the α-dioxocyclopentenyl analogue exists in solution predominantly (70–80%) as the planar 6-s-trans conformer, similar to violerythrine chromophore analogues. In order to identify the minor solution forms, molecular modeling and geometry optimizations using the semiempirical molecular orbital method AM1 defined two additional symmetry-related minima at ±30–40° in its C^6–C^7 torsional energy profile. Because the chromophores of bacterio- and halorhodopsins and sensory rhodopsins are bound as the 6-s-trans conformer [Harbison, G. S., Smith, S. O., Pardoen, J. A., Courtin, J. M. L., Lugtenburg, J., Herzfeld, J., Mathies, R. A., & Griffin, R. G. (1985) *Biochemistry 24*, 6955–6962; Baselt, D. R., Fodor, S. P. A., van der Steen, R., Lugtenburg, J., Bogomolni, R. A., & Mathies, R. A. (1989) *Biophys. J. 55*, 193–196], we suggest that the cyclopentenyl analogue's α-diketo function may be favorably positioned within the binding pocket and sufficiently reactive toward nucleophilic attack to cross-link an arginine located in or near the ring end of the chromophore cavity: Arg^{134} according to the current model of bacteriorhodopsin's tertiary structure [Henderson, R., Baldwin, J. M., Ceska, T. A., Zemlin, F., Beckmann, E., & Downing, K. H. (1990) *J. Mol. Biol. 213*, 899–929] or Arg^{82} as postulated from an alternate model constructed primarily to accommodate the external point charge contribution to bacteriorhodopsin's opsin shift [Spudich, J. L., McCain, D. A., Nakanishi, K., Okabe, M., Shimizu, N., Rodman, H., Honig, B., & Bogomolni, R. A. (1986) *Biophys. J. 49*, 479–483].

Probing the chromophore site of retinal-binding proteins has depended primarily upon studying the interactions of synthetic, conformationally well-characterized retinal analogues with proteins whose tertiary structures are essentially unknown (Balogh-Nair & Nakanishi, 1982; Crouch, 1986; Liu & Mirzadegan, 1988). The solution conformations of the major geometric isomers of retinal are described in the seminal works of Patel (1969), Honig et al. (1971), and Rowan et al. (1974); the crystalline structures for these and some related analogues are also known (Bart & MacGillavry, 1968; Gilardi et al., 1971; Schenk, 1971; Hamanaka et al., 1972; Gieren et al., 1982; Simmons et al., 1986a,b). However, for bacterial rhodopsins at least one of the conformational constraints that shapes the free chromophore in solution and in most crystalline lattices appears to be violated in the protein-bound chromophore. In retinals, the orientation of the ring relative to the polyenal chain is described by the C^5–C^6–C^7–C^8 torsional angle, ϕ^{5678}. In accord with calculated stabilities of the ring–chain conformers (Pullman et al., 1969; Honig et al., 1971), most unbound retinal chromophores exist in solution and crystal as twisted 6-s-cis forms where ϕ^{5678} is between −30° and −80°; protein-bound retinal analogues, however, can exist in the 6-s-trans form where ϕ^{5678} is assumed to be planar (i.e, 180°) as determined by analyses of ^{13}C NMR parameters in solid-state studies of bacteriorhodopsin (bR)[1] (Harbison et al., 1985) and by using the conformationally rigid 6-s-cis- and

* Author to whom correspondence should be addressed. Present address: M&S Data Analysis and Molecular Speculations, P.O. Box 30607, Charleston, SC 29417.
‡ Department of Pharmacology, Medical University of South Carolina.
§ Department of Ophthalmology, Medical University of South Carolina.

[1] Abbreviations: bR, bacteriorhodopsin; NMR, nuclear magnetic resonance; NOE, nuclear Overhauser effect; NOESY, two-dimensional NOE-correlated spectroscopy; COSY, two-dimensional *J*-correlated spectroscopy; AM1, Austin Method 1; $1^{(R,S)}$, prochiral designations of the geminal methyls at C^1 on the retinal ring.

0006-2960/91/0430-2976$02.50/0